

Physical modeling of magma chamber of slamet volcano by means of satellite gravimetric data

Sehah*, Urip Nurwijayanto Prabowo, Sukmaji Anom Raharjo, Aina Zahra Ikhwana

Physics Department, Faculty of Mathematic and Natural Sciences, Jenderal Soedirman University, Purwokerto 53122, Indonesia

Article history:

Received: 12 October 2022 / Received in revised form: 13 December 2022 / Accepted: 15 December 2022

Abstract

Slamet Volcano (3,432 m) is the highest volcano in Central Java, Indonesia with a weak explosive type of eruption compared to other active volcanoes. Physical modeling of magma chamber is very important because it can help to reveal the characteristics of Slamet Volcano eruptions. The modelling used the gravimetric satellite data from GGMplus, which is best in spatial resolution compared to other satellite data, i.e. 220 m. Data processing began with Bouguer correction and terrain correction and resulted in complete Bouguer anomalies data with the values ranging from 11.068 to 117.451 mGal. Further, residual Bouguer anomalies data were obtained after data reduction to the horizontal surface and removal of regional anomalies data to obtain values ranging from -67.569 to 38.808 mGal. The residual anomaly contour map showed the lowest anomalous value under the volcanic cone at positions of 109.21967° E and 7.24281° S as estimated to be the location of the magma chamber of Slamet Volcano. However, the inversion modeling resulting from the residual Bouguer anomalies data showed that the magma chamber of Slamet Volcano can be observed clearly at the positions of 109.22053° E and 7.24719° S. The location of the magma chamber is not perfectly vertical under the volcanic cone but has a slight slope. The obtained model of the magma chamber has a relatively small volume and shallow depth, i.e. about 1 – 4 km. The obtained physical parameters of the magma chamber impact the characteristics of the eruption of Slamet Volcano, which tends to be weak explosive.

Keywords: Magma chamber; Slamet Volcano; satellite gravimetric data; residual anomalies data; physical modeling

1. Introduction

The gravity method is one of the geophysical methods widely used for underground exploration. The principle of this method is to measure the difference in the value of the gravitational field on the Earth's surface, which can be mapped in the form of a gravity anomaly map. Basically, the gravitational field value is not fixed on the Earth's surface, but its value changes due to fluctuations in the density of rocks, especially the subterranean rocks that make up the Earth's crust [1]. The gravitational field values on the Earth's surface are determined by subsurface geological structures, including the uneven topography of the Earth's surface. All geological structures below the surface affect the gravitational field value at the surface [1]. The gravity method can be used to identify types of rock or geological structures based on the fluctuations in the gravitational field [2]. In the field of natural resources exploration, gravity method has been applied to detect the accumulation of certain minerals or mining materials [3]. It can also be applied in disaster preparedness to detect geological structures such as faults or folds, bedrock, intrusions, magma chambers, and aquifers [4]. The use of the gravity method as a monitoring tool for volcanic activity of a volcano is very interesting to study. All the more, the data used for this purpose

is easily accessible and free, like satellite gravimetric data.

Currently, the method for collecting gravity anomalies data is developing rapidly. The process of data acquisition does not have to be done in the field but it can use satellite data. The obtained data will be gravity disturbance data endowed with the geographic position of all points on the Earth's surface. One source of satellite gravimetric anomalies data that can be used for studies is Global Gravity Model plus (GGMplus) [5]. The GGMplus data has several advantages, one of which is better spatial resolution compared to other satellite data on gravitational anomalies such as Topex and BGI data. GGMplus offers data of the Earth's gravity with a resolution of 220 m for all land and coastal areas of our planet between ± 60 degrees latitude [5]. Therefore, the data can be utilized for a preliminary mapping of an area to obtain an overview prior to primary data collection using other geophysical methods. In this study, the GGMplus data have been applied to model the shape of the magma chamber of Slamet Volcano, Indonesia since these data showed good accuracy in interpreting the clues to an area's subsurface structure.

Slamet Volcano (3,432 m) is a stratovolcano located on the boundary of five regencies, i.e. Tegal, Banyumas, Pemalang, Purbalingga, and Tegal regencies, Central Java, Indonesia [6]. Geographically, Slamet Volcano is located at a position of 7°14'30" S and 109°12'30" E. The highest volcano in Central Java has four craters, the fourth of which is the last crater that

* Corresponding author. Tel.: +6281-3275-07517; fax: +62-281-63873.

Email: sehah@unsoed.ac.id

<https://doi.org/10.21924/cst.7.2.2022.1001>

is still active. The last activity with alert status was recorded in August 2019 [7]. The activity of the volcano has been detected since the 19th century and often erupts on a small scale. The eruption of Slamet Volcano occurred during May – June 2009 was marked by the release of magma into lava. Although the alert status has increased in 2019, there has been no catastrophic eruption. The last eruption was recorded in 2014 with a strombolian type [7]. According to information from the Center for Volcanology and Geological Disaster Mitigation Republic of Indonesia, the activity of the Slamet volcano is classified as fluctuating with the type of relatively weakly explosive eruption [8]. The view of Slamet Volcano from the Baturaden, Banyumas Regency is shown in Figure 1.



Fig. 1. The view of Slamet Volcano seen from Banyumas Regency, Central Java, Indonesia

However, there should be alertness for the dangers of volcanic eruptions, considering the high community activity and dense population around the Slamet Volcano. In addition, there are many national assets such as cultural heritage and tourist sites, as well as centers of public economic activities, transportation, agriculture, fisheries, farms, and educational institutions. Hence, a study must be carried out to minimize the negative impacts caused by the eruption of Slamet Volcano. Pre-mitigation measures can be conducted through studies to identify the Slamet Volcano subsurface structure, particularly the magma chamber [9]. The characteristic of the magma chamber of a volcano plays an important role in the processes taking place within it. Therefore, understanding the magma chamber structure of a volcano will help the processes of analyzing and interpreting volcanic activity well and easily.

1.1. Geological review

It is estimated that Slamet Volcano was formed as a result of the subduction process between the Indo-Australian Plate and the Eurasian Plate south of Java Island. The portion of the top of the Indo-Australian Plate, which is subducting under the Eurasian Plate is melting into magma liquid due to very high subsurface temperatures. Fissures in the Eurasian Plate will open a path for magma to slowly rise to the Earth's surface. On the way to the surface, magma can lose its energy while still in the Earth's crust, so that the liquid stops and forms a magma chamber before reaching the surface [10]. Magma is less dense than the surrounding rocks and this allows it to be easily pushed to the earth's surface if there is adequate energy. Magma that comes out of a volcano is called as lava. Pyroclastic material (a mixture of lava and ash) that erupts for a long time during an eruption settles and accumulates to form a volcanic body [11], such as the body of Slamet Volcano.

The dynamics of the magma chamber of Slamet Volcano is

estimated to have been going on since the late Miocene, which is marked by the presence of the Kumbang Formation unit, consisting of volcanic rocks from the terrestrial and marine environments that occupy the central part of Java Island [12]. Based on the geological information, the basement of Slamet Volcano consists of the Halang and Rambatan Formations that are unconformably overlain by volcanic rock deposits of the Kumbang Formation in the late Miocene and greenish coarse sandstone and conglomerate from the Tapak Formation in the Pliocene age. All the tertiary rocks were then covered by lava and alluvium deposits of Slamet Volcano. This indicates that Slamet Volcano, which is a composite stratovolcano grows on the tertiary deposits with a diameter of 50 – 60 km [13]. The rock formations, which make up the body of Slamet Volcano consist of lava deposits and undifferentiated volcanic rocks. The lava of Slamet Volcano consists of highly porous and fractured andesitic lava, whereas the undifferentiated volcanic rocks consist of breccia, lava, and tuff. Both rock formations are Pleistocene in age [14]. Complete geological information can be seen on the geological map, as shown in Figure 2.

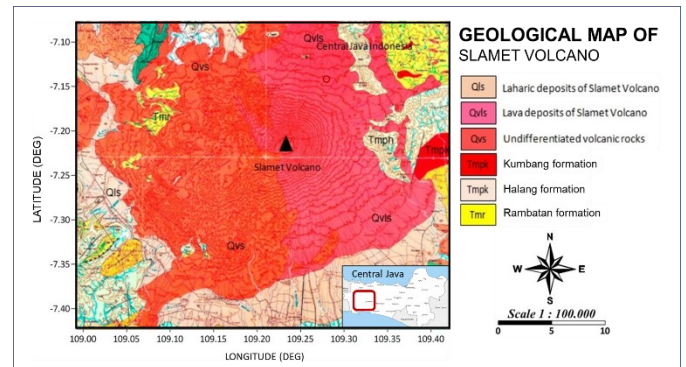


Fig. 2. Geological map of Slamet Volcano and its surrounding areas [15]

1.2. Gravity method review

The gravity survey method is based on the Newton's Law of attraction between two point masses, where the magnitude of the force between m_1 and m_2 separated by a distance r can be written as [16]

$$\vec{F}(\vec{r}) = -G \frac{m_1 m_2}{r^2} \hat{r} \tag{1}$$

where G is the universal gravitation constant ($6.67 \times 10^{-11} \text{ Nm}^2/\text{kg}^2$). Telford et.al. [16] described equation (1), so that the value of the gravitational potential at point P outside the volume V as shown in Figure 3 can be expressed by the equation

$$U_P(\vec{r}) = - \int_V \frac{G}{|\vec{r} - \vec{r}_0|} dm = -G \int_V \frac{\rho(\vec{r}_0)}{|\vec{r} - \vec{r}_0|} d^3\vec{r}_0 \tag{2}$$

where $|\vec{r} - \vec{r}_0| = \sqrt{r^2 + r_0^2 - 2r r_0 \cos \gamma}$

If the volume integral is taken for the entire volume of the Earth, the gravitational potential at the Earth's surface can be obtained. The gravitational field can then be obtained by differentiating the gravitational potential so that the equation is presented as follows.

$$\vec{E}(\vec{r}) = |-\nabla U_P(\vec{r})| \tag{3}$$

The earth's gravitational field value is often referred to as the gravitational acceleration and is given with the symbol g . Based on equation (2) and equation (3), the value of the Earth's gravitational field can be expressed by equation [16]

$$g(\vec{r}) = |-\vec{E}(\vec{r})| = |\nabla U_P(\vec{r})| \tag{4}$$

equation (4) can be stated more fully into equation (5) as seen in the equation [16]

$$g(\vec{r}) = -G \int_V \frac{\rho(\vec{r}_0) z d^3 \vec{r}_0}{(x^2 + y^2 + z^2)^{3/2}}$$

$$g(\vec{r}) = -G \int_V \frac{\rho(\vec{r}_0)(z_0 - z) d^3 \vec{r}_0}{[(x - x_0)^2 + (y - y_0)^2 + (z - z_0)^2]^{3/2}} \tag{5}$$

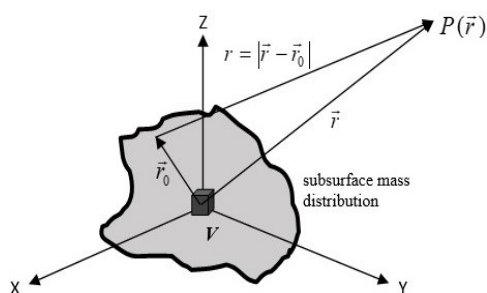


Fig. 3. The gravitational potential at point P on the Earth's surface due to the continuous distribution of mass in the subsurface [16]

equation (5) indicates that the value of the earth's gravitational field changes with latitude, longitude, altitude and the distribution of subsurface body densities. This means that the gravitational field at the Earth's surface is influenced by subsurface rocks of different densities. Fluctuations in the gravitational field at the Earth's surface are also determined by geological structures and uneven relief of the Earth's surface (rough topography). In a gravity survey method, the value of the gravitational field, which is the result of data collection, is given in units of gal, where 1 gal equals to 10^{-5} m/s^2 . In general, the gravity anomalies data in the field are very small, in the milligal range [1].

2. Materials and Methods

2.1. Location of research

This study was conducted at the Laboratory of Geophysics, Department of Physics, Faculty of Mathematics and Natural Sciences, Jenderal Soedirman University, Purwokerto, Central Java, Indonesia. The geophysical data used in this study were satellite gravity anomalies data covering Slamet Volcano and the surrounding area in the position of $108.993^\circ - 109.401^\circ \text{ E}$ and $7.021^\circ - 7.403^\circ \text{ S}$ as shown in Figure 4. Administratively, the study area is located on the border of Pemalang, Brebes, Tegal, Banyumas, and Purbalingga Regencies, Central Java, Indonesia.

2.2. Equipment, and materials

The equipment used for this study included a personal computer, equipped with Microsoft Excel 2019 and Plato 4.75

for data processing, Surfer 17 for data mapping, and Grablox 1.7 for data modeling. While the materials used for this research included gravity disturbance data from GGM plus which are equivalent to free-air gravity anomalies data [17,18]. The data also were equipped with topography and geoid data for all observation points in the study area. GGMplus data with 220 m resolution was found much better than Topex data with 1.85 km resolution [5].

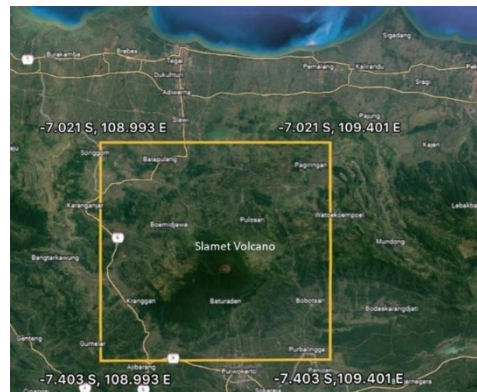


Fig. 4. Location of study area; Slamet Volcano and its surrounding area (Source; Google Earth) [18]

2.3. Research procedure

The study began by accessing gravity field data from the GGMplus, i.e. gravity disturbance data. The data were accessed from the website as provided by Bureau Gravimetric International [19]. The data have been downloaded and stored by the Microsoft Excel. The obtained gravity disturbance data have been equipped with topography and geoid data at each observed point on the earth's surface. The gravity disturbance data required no free-air correction because the acquisition was carried out at the same elevation datum [20]. The latitude correction was also not required in the data processing because the satellites calculated the differences effect in latitude positions on the gravity values. In addition, the distance from the earth center of mass to the satellite orbital trajectory is large, so the difference in the gravity disturbance caused by the difference in latitude will not have much effect [21]. Some corrections commonly applied to the gravimeter such as equipment elevation correction and drift correction were also not required [21]. Hence, it was only Bouguer and terrain corrections applied in data processing to obtain Complete Bouguer Anomaly (CBA) data [22] representing the presence of areas of locally high or low density in the subsurface of the Earth [23,24].

Actually, CBA data are still distributed on the topographical surface that are a function of longitude, latitude, and altitude. The reduction of CBA data to a horizontal surface must be carried out to proceed the data can at the succeeding stage [25]. The method applied to reduce CBA data to a horizontal surface is the equivalent source technique [25]. The CBA data, which have been distributed on the horizontal surface are still affected by subsurface densities originating from the deep and wide sources that are called as regional gravity anomaly. Thus, the regional gravity anomaly must be separated from the CBA data to obtain the residual Bouguer anomalies data [26][27]. The regional Bouguer anomalies data are obtained by means an upward continuation technique, so that the anomalous data

interval becomes very small and the contour pattern is very smooth [28]. Further, the obtained regional Bouguer anomalies data were separated from the CBA data to obtain the residual Bouguer anomalies data. The residual anomalies data were assumed to come from the local subsurface structures and rocks as the target of the study [29].

The local subsurface structure of a volcano consists of lava deposits, pyroclastic materials, and magma chambers. In this study, the target of modeling was the magma chamber because knowing the model and physical properties of the magma chamber might make it easier for explaining and describing the volcanic activity of Slamet Volcano. Here, the researchers used inversion modeling to visualize the model of the magma chamber of Slamet Volcano. For inversion modeling, density parameters were directly calculated using numerical methods from residual gravity anomalies data [30].

3. Results and Discussion

3.1. Results of processing data

Access to GGMplus data has produced gravity disturbance data, equivalent in value to free-air gravity anomaly data [31]. There were 39,360 accessed gravity anomalies data with 220 m resolution, better than the Topex data with 1.85 km resolution. The obtained gravity anomalies data had the values in a range of 27.345 – 322.642mGal. The data were distributed in the study area with the geographical position of 108.993° – 109.401° E and 7.021° – 7.403° S, and elevation in the range of -4.9 – 3,380.8 m. Figure 5 shows the gravity disturbance contour map of the study area. The high anomaly was seen concentrated in the center of the study area, especially under the crater of Slamet Volcano.

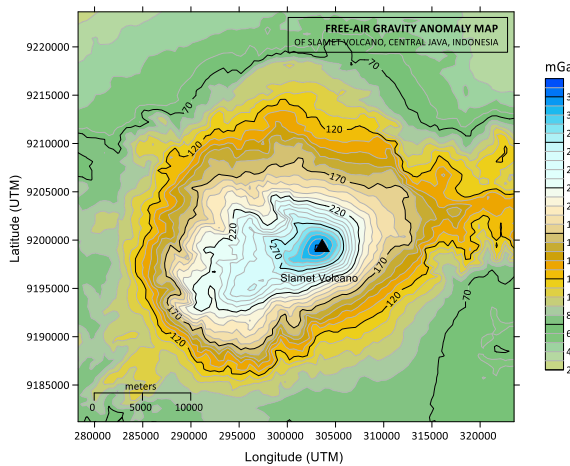


Fig. 5. The gravity disturbance contour map of study area

To obtain the complete Bouguer anomalies (CBA) data, the Bouguer and terrain corrections have been applied to the gravity disturbance data. The Bouguer correction was used to eliminate the mass effect located between the measurement points on the topographic surface to the datum, which was not taken into account even though this mass greatly affected the gravity anomaly data [32]. Meanwhile, the purpose of terrain correction was to eliminate the mass influence around the measurement point. The terrain correction arose due to the change of the topography on the gravitational field at the measurement point. The terrain correction has been calculated

using the Hammer Chart method [33,34]. The values of CBA data ranged from 11.068 – 117.451mGal with the contour map as shown in Figure 6.

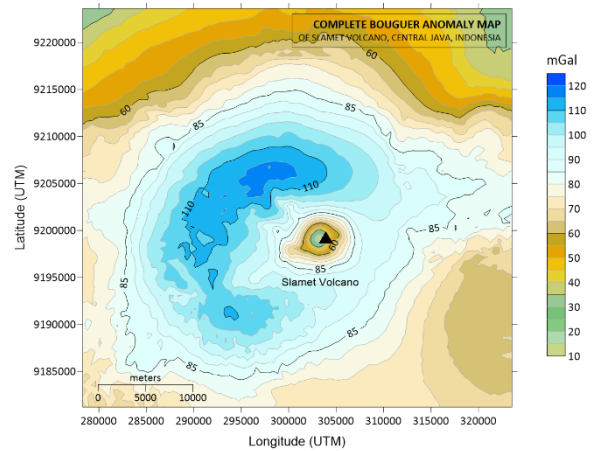


Fig. 6. The complete Bouguer anomalous (CBA) contour map of study area

The CBA data still distributed on the topographic need to be projected to a horizontal surface. The equivalent source technique has been applied for this aim by taking the average topographic height of the study area, i.e. 572.58 m. The CBA data that has been spread at the average topographic elevation ranging from 11.889 to 117.429mGal. The CBA data is superposition of regional and local anomalous sources, such that regional and residual anomalies data are separated; since the target of the study is a magma chamber which is a local anomalous source. The separation of regional anomaly data from CBA data was carried out using the upward continuation technique [35], as described in Research Procedure. When the upward continuation is higher, the local anomalous patterns is getting lost and the regional anomalous patterns are getting stronger [36]. The visual analysis of the anomalous contour maps from the upward continuation showed that the anomalous map at an altitude of 30,000 m tended to remain with a smooth pattern. The contour pattern did not change when upward at an altitude of 35,000 m with an accuracy of 0.0001 m. Hence, the anomalies data were taken as regional anomalies data with values ranging from 77.805 to 78.712mGal. The contour map can be seen in Figure 7.

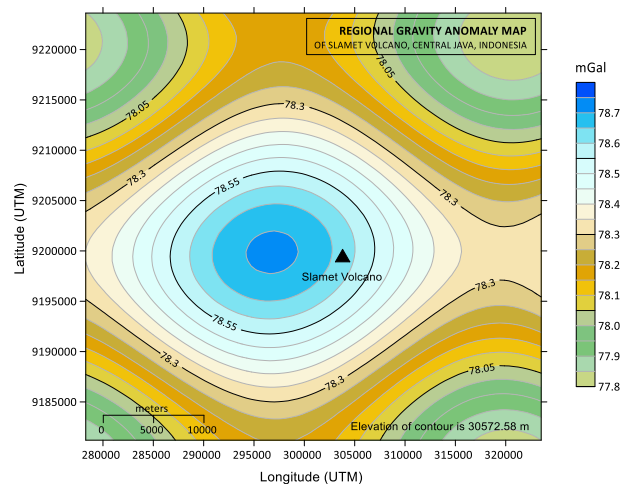


Fig. 7. The regional Bouguer anomalous contour map of study area

The obtained regional anomalies data have been separated from the CBA data distributed in the average topographical height. This process has resulted in residual Bouguer anomalies data that were also at the average topographic height; i.e. 572.58 m [25] with values in the range of -67,569 to 38,808mGal. The residual Bouguer anomalous contour map is shown in Figure 8. Based on this map, the residual anomalous map tended to show the local patterns. The lowest anomalous value at the position of 109.21967°E and 7.24281°S could be interpreted as the magma chamber of Slamet Volcano. The lower value of the residual anomalous compared to the surrounding area indicated that the magma chamber had a low density. In general, magma with low density is characterized as liquid or molten.

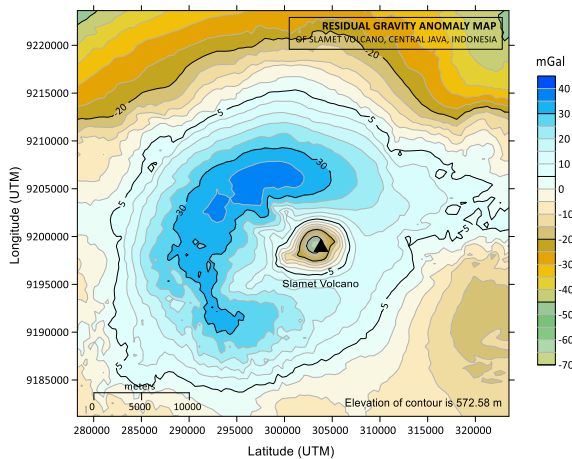


Fig. 8. The residual gravity anomaly contour map of study area

3.2. Results of modeling and interpretation

The inversion modeling of the subsurface structure of Slamet Volcano has been carried out to a depth of 5,000 m below the average topographical height of the study area, i.e. 572.58 m. Before the modeling, the residual anomaly [37] contour map was cut according to the position boundaries of the map area to be modeled as shown in Figure 9. The results of the modeling on the trajectories of L-01 to L-08 obtained are shown in Figure 10 to Figure 17. Based on the modeling results, the magma chamber of Slamet Volcano was interpreted as being under the volcanic cone and had a density value lower than the average density of rocks in the earth's crust, which is in the range of 1.50 – 1.88 g/cm³. The average density of the continental crust rocks used was taken as 2.67 g/cm³ [38].

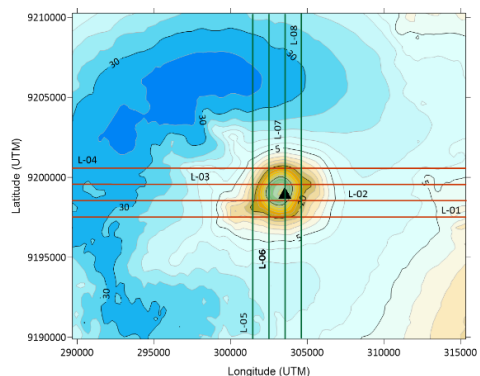


Fig. 9. The residual gravity anomaly contour map which has been cut to the modeling boundaries. This contour is equipped by track of AB and CD used as input data for invers modeling

The modeling results of the residual anomalies data as shown in all figures showed that the model of the magma chamber of Slamet Volcano could be observed most clearly at the positions of 303.530 km-UTM and 9,198.540 km UTM or 109.22053° E and 7.24719° S. The depth of the magma chamber was thought to be in the range of 1 – 4 km below the average topographic surface. The position of the magma chamber observed was not perfectly vertical under the cone of the Slamet Volcano, but had a slight slope. The cone of Slamet Volcano is located at geographical position of 109.21661° E and 7.24308° S. These results are in accordance with the results of studies on the identification of the magma dynamics based on the volcanic tremor analysis of Slamet Volcano [39]. When the modeling results on the L-01 to L-04 were correlated, the magma chamber of Slamet Volcano had a diameter of more than 3.06 kilometers in the north-south direction. While, when the modeling results on the L-05 to L-08 were correlated, the diameter of the magma chamber was more than 3.08 kilometers in the west-east direction.

3.3. Discussion

The residual Bouguer anomalous contour map (as shown in Figure 8) shows the presence of the old Slamet Volcano complex in the west to northwest. Most of these areas are characterized by high anomaly that are interpreted as buried andesitic lava resulting from the eruption of the old Slamet Volcano. All the rocks have been covered by undifferentiated volcanic rocks, including volcanic breccia, lava and tuff with its distribution form of flat and hilly areas [15]. Further, the areas in the south, southeast, east and southwest are the volcanic rock complexes of the medium Slamet Volcano, dominated by moderate to low anomaly values. Meanwhile, the areas in the north, northeast, and a small portion of the west are the rock complexes of the young Slamet Volcano [12], which are characterized by high, medium, and low anomaly values. The young Slamet Volcano complexes are composed of pyroclastic breccia and erupted lava. On the lower slopes of the old Slamet Volcano, many geothermal manifestations also appear. These manifestations appear in the volcanic rocks and bedrock in the form of sandstone-claystone [40]. Based on the observation results, the geothermal surface manifestation followed a distinct fault pattern with a northwest-southeast trend that bisected the old Slamet Volcano body [41].

All subsurface anomalous models (as shown in Figure 10 to Figure 17) showed the magma flow of Slamet Volcano from below Earth's crust to the surface of the volcano. The upward flow of magma occurs due to pressure and buoyancy forces, such that magma will fill the chamber at a relatively shallow depth. The continuous filling of magma causes the pressure in the magma chamber to increase. Increasing pressure in the chamber for a long time will cause magma to try to find its way to the earth's surface to release the pressure through weak zones in the rock layers above. Several of the magma push through vents and fissures to the Earth's surface. Magma that has erupted from a volcano is called as lava.

Based on the data from the Geological Agency of Republic of Indonesia, the eruption characteristic of Slamet Volcano is weak explosive and sometimes just a lava flow accompanied by the eruption of ash and scoria [42]. Generally, this eruption type indicates that the depth of the magma chamber of Slamet

Volcano is shallow [43]. This is in accordance with the results of this study that found the depth of the magma chamber of Slamet Volcano in the range of about 1 - 4 kilometers under the average topographical elevation. The results of this study are also in accordance with data from the Center for Volcanology Mitigation and Geological Hazards [43], which stated that the depth of the magma chamber of Slamet Volcano is not more than 2 km, even if the volcanic activity increases, magma can rise to a depth of 1 km below the crater. The gases that come out from the shallow magma chamber are relatively easy, so that magma can come out of the volcano relatively without a gas explosion. A good example is the eruptions of Slamet volcano. The Slamet Volcano eruptions tend to be effusive that are characterized by the flow of lava from the volcano craters to the ground, and sometimes accompanied by small explosive eruptions [44].

In addition, the modeling results showed that the volume of the magma chamber of Slamet Volcano is not so large, so the volume of high-pressure gas that pushes magma to the surface is relatively small [45]. Therefore, the releasing process of magma to the Earth's surface through volcanic craters does not occur with very strong pressure (not accompanied by explosions). Lava flows rarely kill people because they move quite slowly for people to get out of their way. Based on the records, the eruption of Slamet Volcano was first observed on August 11-12, 1772 and had never caused any casualties [46]. The results of the study and discussion (in this paper) indicated that the shallow depth and the small volume for the magma chamber are the main key to reveal the characteristics of the eruption of Slamet Volcano, which tends to be weak explosive and sometimes lava flows accompanied by small explosions of ash and scoria [42].

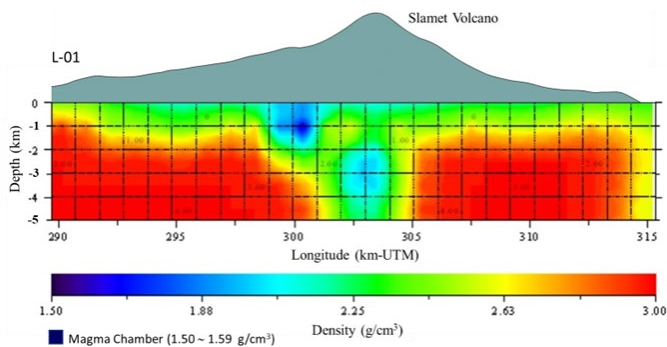


Fig. 10. A cross-section of the anomalous object model along L-01 trajectory at latitude of 9,197.520 km-UTM

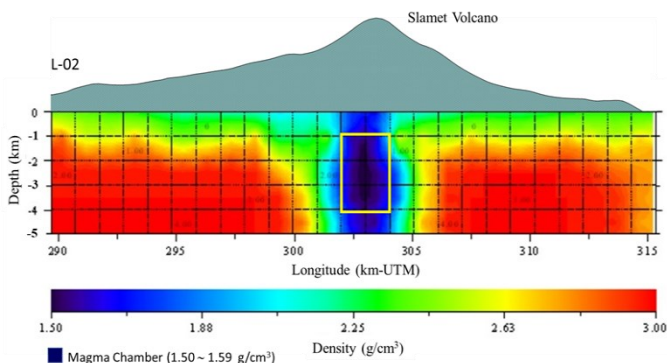


Fig. 11. A cross-section of the anomalous object model along L-02 trajectory at latitude of 9,198.540 km-UTM

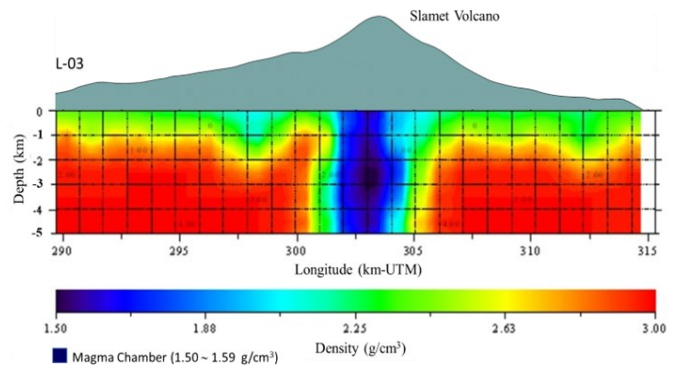


Fig. 12. A cross-section of the anomalous object model along L-03 trajectory at latitude of 9,199.560 km-UTM

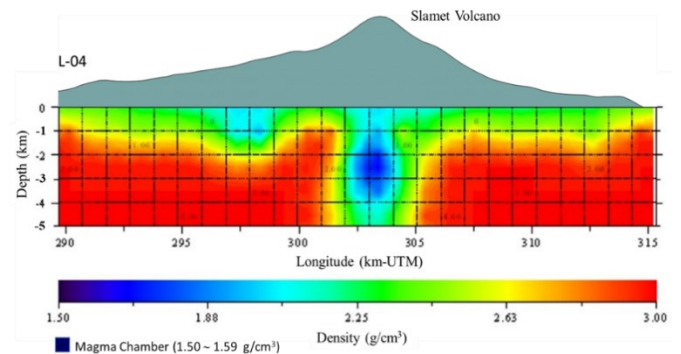


Fig. 13. A cross-section of the anomalous object model along L-04 trajectory at latitude of 9,200.580 km-UTM

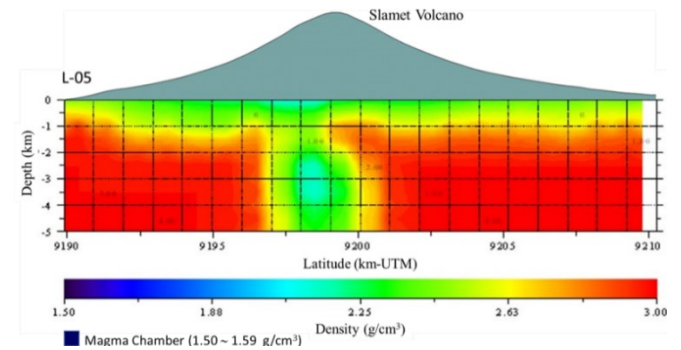


Fig. 14. A cross-section of the anomalous object model along L-05 trajectory at longitude of 301.470 km-UTM

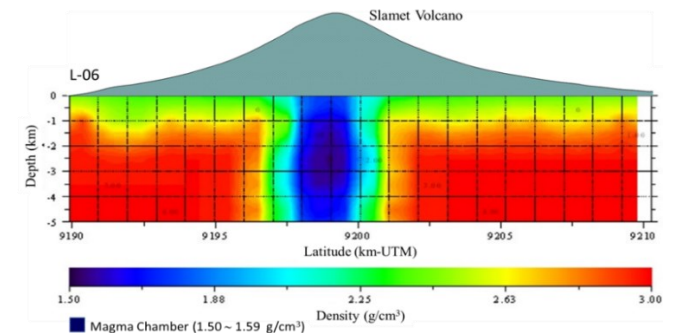


Fig. 15. A cross-section of the anomalous object model along L-06 trajectory at longitude of 302.500 km-UTM

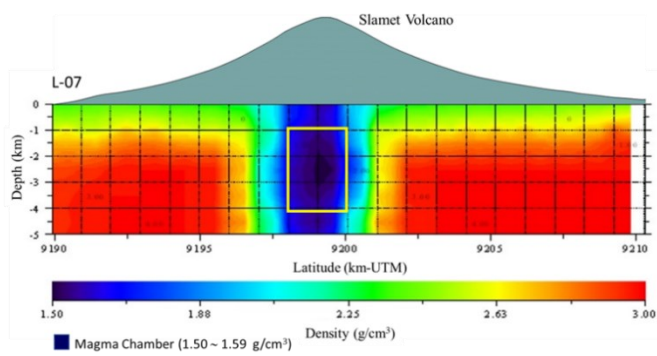


Fig. 16. A cross-section of the anomalous object model along L-07 trajectory at longitude of 303.530 km-UTM

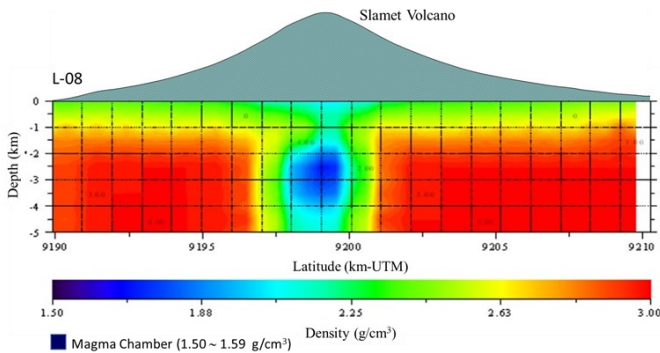


Fig. 17. A cross-section of the anomalous object model along L-08 trajectory at longitude of 304.550 km-UTM

4. Conclusion

The physical modeling of the Slamet volcano magma chamber, Central Java, Indonesia, by means of the satellite gravimetric data has been successfully done. The gravimetric satellite data used was GGMplus data, which has the best spatial resolution compared to other satellite data. After several corrections were applied to the gravity disturbance data, then the complete Bouguer anomalies (CBA) data could be obtained with values in the range of 11,068 to 117,451 mGal. While, the residual Bouguer anomalies data were obtained after applying reduction to the horizontal surface and separation of the regional anomalies data with values in the range of -67.569 to 38.808 mGal. The residual anomalous contour map showed that the lowest gravity anomaly value is located under the volcanic cone at a position of 109.21967° E and 7.24281° S, which was predicted to be the location of the magma chamber of Slamet Volcano, which is currently still active. But the results of the inversion modeling of the residual Bouguer anomalies data indicated that the model of the magma chamber of Slamet Volcano can be most clearly observed at the positions of 109.22053° E and 7.24719° S. This magma chamber position is not perfectly vertical below the volcanic craters, but has a slight slope. The obtained model of the magma chamber of Slamet Volcano has a relatively small volume and shallow depth. This obtained model is in accordance with the characteristics of the eruption of Slamet Volcano, which tend to be weak explosive, and sometimes effusive in the form of lava flows accompanied by small explosions.

Acknowledgements

The authors would like to thank the Institute for Research and Community Service of Jenderal Soedirman University for

providing the research funding. The authors also express a gratitude to the research group members for their cooperation from accessing to interpreting data.

References

1. G. Balmino, and S. Bonvalot. *Gravity Anomalies*. Encyclopedia of Geodesy. Springer International Publishing Switzerland. 2016.
2. L. Hasanah, A. Aminudin, N. D. Ardi, A. S. Utomo, H. Yuwono, Kamtono, D. D. Wardhana, K. L. Gaol, and M. Iryanti. *Graben Structure Identification Using Gravity Method*. In IOP Conf. Series: Earth and Environmental Science, 29 (2016) 012013.
3. A. Vincent, M. Kassim, M. Charles, A. Willis, M. Gerald. *Geophysical Exploration of Iron Ore Deposit in Kimachia Area in Meru County in Kenya, Using Gravity and Magnetic Techniques*. Int. j. sci. res. publ., 2 (2013) 104-105.
4. Y. L. Ekinci, and E. Yigitbas. *Interpretation of Gravity Anomalies to Delineate Some Structural Features of Biga and Gelibolu Peninsulas, and their Surroundings (North-West Turkey)*. Geodin. Acta, 27 (2015) 300-319.
5. M. Chamaco, and R. Alvarez. *Geophysical Modeling with Satellite Gravity Data: Eigen-6C4 vs GGM Plus*. engr., 13 (2021) 690-706.
6. I. Pratomo and M. Hendrasto. *Eruption Characteristics of Mount Slamet, Central Java. Mount Slamet Ecology: Geology, Climatology, Biodiversity and Social Dynamics*. Biology Research Center – LIPI in collaboration with Jenderal Sudirman University. 2012.
7. A. Harijoko, A. N. Milla, H. E. Wibowo, and N. I. Setiawan. *Magma Evolution of Slamet Volcano, Central Java, Indonesia Based on Lava Characteristic*. IOP Conf. Ser.: Earth Environ. Sci., 451 (2020) 012092.
8. I. S. Sutawidjaja and R. Sukhyar. *Cinder cones of Mount Slamet, Central Java, Indonesia*. Indones. J. Geosci., 4(1) (2009) 57-75.
9. M. Fedi, F. Cella, M. D. Antonio, G. Florio, V. Paoletti, and V. Morra. *Gravity Modeling Finds a Large Magma Body in the Deep Crust below the Gulf of Naples, Italy*. Sci. Rep., 8 (2018) 1-19.
10. A.F. Glazner. *Climate and the Development of Magma Chambers*. Geosciences., 10 (2020) 93.
11. S. Gharehchahi, *Volcanic Processes and Landforms*, The International Encyclopedia of Geography. John Wiley & Sons Ltd. 2017.
12. I. Pratomo. *Geological Diversity of the Mount Slamet Volcanic Complex, Central Java. Mount Slamet Ecology: Geology, Climatology, Biodiversity and Social Dynamics*. Biology Research Center-LIPI in collaboration with Jenderal Sudirman University. 2012.
13. F. Sangaji, N. L. Sidik, F. Wowa, and F. R. Rianti. *Geology and Facies of Slamet Volcano based on Volcanostratigraphic and Geomorphological Analysis and their Implications for the Geology of the Environmental Management of the Belik Region and Surrounding Areas, Belik District, Pemalang Regency, Central Java*. In Proceedings 10th National Seminar on Earth: The Role of Earth Sciences in Infrastructure Development in Indonesia. Yogyakarta, 13 – 14 September 2017, (2017) 1381-1394.
14. I. S. Sutawidjaja, D. Aswin, and K. Sitorus. *Geologic Map of Slamet Volcano, Central Java*, Vulcanological Survey of Indonesia, Bandung. 1985.
15. M. Djuri, H. Samodra, T. C. Amin, and H. Gafoer. *Geological Map of The Purwokerto and Tegal Quadrangles Jawa*. Geological Research and Development Center. Bandung. 1996.
16. W. M. Telford, L. P. Gedaart, and R. E. Sheriff. *Applied Geophysics*. Cambridge. New York. 1990.
17. A. Suprianto, Supriyadi, N. Priyantari, and B. E. Cahyono. *Correlation Between GGMplus, Topex and BGI Gravity Data in Volcanic Areas of*

- Java Island. Journal of Physics: Conference Series, 1825 (2021) 012023.
18. Trapsilawati, F., Wijayanto, T., & Jourdy, E. S. *Human-computer trust in navigation systems: google maps vs waze*. Commun. Sci. Technol. 4 (2019) 38-43.
 19. R. Apriliani, R. D. Indriana, U. Harmoko, and T. Yulianto. *The GGMplus Data Analysis for Modeling of the Kelimutu Volcanic Subsurface*. IJSHRE., 6 (2021) 9-15.
 20. M. Yanis, Marwan, and N. Ismail, *Efficient Use of Satellite Gravity Anomalies for Mapping the Great Sumatran Fault in Aceh Province*. Indones. J. Appl. Phys., 9(2) (2019) 61-67.
 21. A. D. Maulana and D. A. Prasetyo. *Mathematical Analysis on Bouguer Correction and Field Correction on Topex Satellite Gravity Data and Application in Geohazard: A Case Study of the Palu Koro Fault, Central Sulawesi*. Jurnal Geosaintek, 5 (2019) 91-100.
 22. D. R. Putri, M., Nanda, S., Rizal, R. Idroes, and N., Ismail. *Interpretation of Gravity Satellite Data to Delineate Structural Features Connected to Geothermal Resources at Bur Ni Geureudong Geothermal Field*. IOP Conf. Ser.: Earth Environ. Sci., 364 (2019) 012003.
 23. S. Wada., A. Sawada, Y. Hiramatsu, N. Matsumoto, S. Okada., T. Tanaka, and R. Honda. *Continuity of Subsurface Fault Structure Revealed by Gravity Anomaly: The Eastern Boundary Fault Zone of The Niigata Plain, Central Japan*. Earth Planets Space, 69 (2017) 1-12.
 24. M. N. A. Zakariah, N. Roslan, N. Sulaiman, S. C. H. Lee, U. Hamzah, K. A. M. Noh, and W. Lestari. *Gravity Analysis for Subsurface Characterization and Depth Estimation of Muda River Basin, Kedah, Peninsular Malaysia*. Appl. Sci., 11 (2021) 6363.
 25. R. J., Blakely. *Potential Theory in Gravity and Magnetic Applications*. Cambridge University Press. New York. 1995.
 26. L. Zhaohui, Z. Qiang, W. Yangang, Y. Changbao, Z. Guoxing, and X. Gongcong. *Application of Several Potential Field Separation Methods of Gravity Data in Vientiane of Laos Area*. Global Geology, 20 (2017) 89-97.
 27. L. Guo, X. Meng, Z. Chen, S. Li, and Y. Zheng. *Preferential Filtering for Gravity Anomaly Separation*. Comput. Geosci., 5 (2013) 247-254.
 28. E. Minarto, B. J. Santosa, Faridawati, N. Y. Azhari, T. Widihartanti, and Y. L. A. Titi. *Regional Bouguer Anomaly Gravity Data: 3-D Modelling of Subsurface Structures of The Flores and Timor Earthquake Risk Area*. J. Phys. Conf. Ser., 1825 (2021) 012017.
 29. S. O. Eteje, O. F. Oduyebo, P. D. Oluyori. *Modelling Local Gravity Anomalies from Processed Observed Gravity Measurements for Geodetic Applications*. IJSRST, 6 (2019) 144-162.
 30. K. S. Essa, *A Fast Interpretation Method for Inverse Modeling of Residual Gravity Anomalies Caused by Simple Geometry*, J. Geol. Res., (2012) 327037.
 31. C. Hirt, S. J. Claessens, T. Fecher, M. Kuhn, R. Pail, and M. Rexer. *New Ultrahigh - Resolution Picture of Earth's Gravity Field*, Geophys. Res. Lett., 40 (2013) 4279-4283.
 32. P. Zahorec and J. Papco. *Estimation of Bouguer Correction Density Based on Underground and Surface Gravity Measurements and Precise Modelling of Topographic Effects - Two Case Studies from Slovakia*. Contrib. Geophys. Geod., 48 (2018) 319-336.
 33. S. Hammer. *Terrain Corrections for Gravimeter Stations*. Geophysics, 4 (1939) 184-194.
 34. S. Jahanjooy, M. Pirouei, and K. Kolo. *High Accuracy Gravity Terrain Correction by Optimally Selecting Sectors Algorithm Based on Hammer Charts Method*. Stud. Geophys. Geod., 6 (2020) 172-185.
 35. H. Kebede, A. Alemu, and S. Fisseha. *Upward Continuation and Polynomial Trend Analysis as a Gravity Data Decomposition, Case Study At Ziway-Shala Basin, Central Main Ethiopian Rift*. Heliyon, 6 (2020) e03292.
 36. H. Gabtni, C. Jallouli. *Regional-Residual Separation of Potential Field: an Example from Tunisia*. J. Appl. Geophy., 137 (2017) 8-24.
 37. A. Biswas. *Interpretation of Residual Gravity Anomaly Caused by Simple Shaped Bodies Using Very Fast Simulated Annealing Global Optimization*. Geosci. Front., 6 (2015) 875-893.
 38. W. J. Hinze, *Bouguer reduction density, why 2.67?*. Geophysics, 68(5) (2003) 1559-1560.
 39. W. Lumbanraja, and K. S. Brotopuspito. *Identification of Magma Dynamics Based on Volcanic Tremor Analysis at Slamet Volcano, Central Java*. J. Fis. Indones., 19 (2015) 55-61.
 40. A. Widagdo, A. Candra, S. Iswahyudi, C.I. Abdullah. *The Influence of the Geological Structure of Young and Old Mount Slamet on Geothermal Distribution Patterns*. Proceeding: 4th Industrial Research Workshop and National Seminar (IRWNS), (2013) 204-207.
 41. S. Iswahyudi, I. Permanajati, R. Setijadi, J. A. Zaenurrohman, and M. A. Pamungkas, 2020. *Origin of Geothermal Water Around Slamet Volcano, Paguyangan, Cipari, Central Java, Indonesia*. JGEET, 5 (2020) 181-184.
 42. Sumarwoto. *ESDM: The Character of Mount Slamet's Eruption Weakens*. 2002.
 43. Sumarwoto. *Slamet Volcano Magma is Approaching the Surface of the Crater*. 2014.
 44. I. Rusydy. *Melek Bencana: Prepare Knowledge Before Disaster, Get to Know Slamet Volcano Closer*. 2014.
 45. D. Vukadinovic and I. Sutawidjaja. *Geology, Mineralogy and Magma Evolution of Gunung Slamet Volcano, Java, Indonesia*. J. Southeast Asian Earth Sci., 11 (1995) 135-164.
 46. Kabar24. *Mount Slamet Alert: Since 1772-Present It Has Never Taken A Victim*. 2014.